Spaceborne and under-satellite laser sensing of aerosol and cloud fields of troposphere

Yu.S. Balin, S.V. Samoilova, and I.E. Penner

Institute of Atmospheric Optics,
Siberian Branch of the Russian Academy of Sciences, Tomsk

Received February 19, 2007

The activity of the Institute of Atmospheric Optics in the sphere of space instrument designing the first Russian lidar "BALKAN" for the orbital station "Mir," in creation of methods for interpreting data of space laser sensing of crystalline and water cloud formations is described. The results of observation of troposphere in the period of forest fires in 2006 year with the use of the ground-based lidar "LOZA-S" (IAO SB RAS) and space lidar CALIPSO (USA) are presented.

Since appearance in 1963 of the first pioneer paper by G. Fiocco and L.D. Smullin devoted to the study of scattering layers in the upper atmosphere with the use of optical lidars, a significant progress has been reached in application of these modern instruments for remote monitoring of aerosol, gas composition, as well as optical and meteorological parameters of the atmosphere.

Suffice it to say that development of lidar technique made it possible to pass now to permanent atmospheric observations and to create a number of large lidar networks. The NDACC (Network for the Detection of Atmospheric Composition Change), united 16 lidar stations around the world,[1] is intended for monitoring of ozone, aerosol, temperature, and humidity aiming at the study of climatic problems. The MPL-Net based on micropulse lidars[2] is developed under the aegis of NASA for monitoring of tropospheric aerosol. The European EARLINET (European Aerosol Research Lidar Network),[3] created in 2000 year, coordinates the operation of more than 20 lidar complexes of European countries, monitoring the large-scale transfer of aerosol admixtures, mainly from the region of Sahara desert.

This modernized network under the name EARLINET-ASOS in 2006 took part in new 5-year project aimed at optimization and standardization of instrumentation, as well as constructing a common database.[2] Lidar investigations of the dust aerosol emission from desert territory of China were carried out in the framework of the Asian Dust Network (AD-Net)[4]. The Regional East Atmospheric Lidar Mesonet (REALM)[5] and lidar network in Latin America[6] are now under development. Regular monitoring of atmospheric aerosol and ozone in CIS is carried out since 2006 using the network of lidar stations CIS-LiNet[7] located in Russia, Belarus, and Kyrgyzstan. The tendency of development of regional lidar networks takes a planetary character, and the problem of construction of the World lidar network GALION (GAW Aerosol Lidar Observation Network) is now in the order of the day.

In this connection, the organization of spaceborne lidar observations is natural. In 70th, the International working group under the direction of NASA was created, which at the first stage has planned to solve a series of basic scientific problems by means of the spaceborne lidar.[8] The first space lidar was launched by NASA in 1994 onboard "Shuttle" under the program Lidar In-space Technology Experiment (LITE). The results of these experiments were discussed at numerous lidar conferences. The 11-day flight of the lidar has opened new prospects in the remote laser sensing of the atmosphere from the space orbit. The development of new technologies became the basis for constructing of the specialized automated lidar satellite CALIPSO (Cloud Aerosol Lidar and Infrared Pathfinder Observations). The spaceborne instrumentation, created in cooperation by specialists of America (NASA, lidar CALIOP) and French (CNES, infrared radiometer and wide-angle videocamera) was launched to the near-earth orbit in spring, 2006. Now it provides for vast amount of data on aerosol and cloud fields in the atmosphere over the whole territory of the planet.[9]

The Institute of Atmospheric Optics SB RAS also takes an active part in national and international space programs covering the space instrumentation design, theoretical methods for the sensing data interpretation, as well as immediate participation in the satellite experiments, including their validation with ground-based lidars. In this paper we present some aspects of the Institute of Atmospheric Optics activity in this field during the last decade.

Spaceborne lidar "BALKAN"

The early efforts to construct a space lidar were undertaken at IAO SB RAS as long ago as 1975. However, only in 1984, the development work on constructing new scientific instrumentation for multi-functional orbital station "Mir" was started to order of the scientific-production association "Energia" (now Russian Space Corporation). The lidar "BALKAN"

0235-6880/07/09 767-06 $02.00

(aerosol lidar complex of The Academy of Sciences) was produced at the Specialized Design Bureau "Optika" of SB AS of the USSR in cooperation with the Scientific-Research Institute of Space Instrument-making. All ground-based tests were finished in 1990, and the lidar was prepared to launching into space as a part of the module "Spektr" of the orbital station "Mir" as it was declared[10] for the first time at the 15th International lidar conference held in Tomsk in July, 1990. However, because of the financial problems, the lidar after retesting was launched into orbit only in May, 1995. The first work cycle was carried out in August–September, 1995. The experiments were planned and realized in the Mission Control Center of Russian Space Agency "Energia" (Korolev town).

The lidar "BALKAN" was intended for the following space experiments:

a) examination of instrumentation potentiality at sensing of clouds and underlying surface;

b) measurement of the global distribution of cloud formations;

c) selection (in combination with passive sensing tools) of different types of cloudiness against the background of the underlying surface;

d) sensing of the ocean upper layer;

e) validation of the station "Mir" orbit parameters using the method of laser sensing.

In its general design principle, "BALKAN"[11] was the typical lidar complex consisting of a set of the following blocks: receiver-transmitter, geodesic range-meter module, the system for recording the lidar signals, instrumentation control panel for cosmonauts. The set of ground-based controlling-testing instrumentation[12] was of importance, providing for examination of the lidar technical parameters during a long cycle of ground-based tests simulating different impact factors of the ambient medium (mechanical, climatic, electromagnetic, etc.) at the step of preparation to the launch, during the launch, and during the space flight.

The main specifications of the lidar are given below.

Wavelength, nm	532
Pulse energy, mJ	0.20
Pulse duration, ns	12
Pulse repetition rate, Hz	0.18
Diameter of the transmitting collimator, mm	120
Divergence of the transmitted laser beam, mrad	0.15
Diameter of the receiving telescope, mm	275
Angle of the field of view, mrad	0.44
Width of transmission band of the interference light filter, nm	3
Quantum efficiency of PMT, %	13
Level of threshold light power of the receiving path, W	$2 \cdot 10^{-8}$
Band width of the electron amplifier, MHz	40
Error of the range meter channel, m	0.75
Width of ADC, bit	6
Temporal resolution of ADC, ns	20
Power, W	200
Lidar mass, kg	120

The receiver-transmitter device of the lidar (Fig. 1) was designed as a unit block, which provided for the necessary hardness and parallelism of the optical axes with the error of no more than 10 angular seconds for the exploitation period. The receiver-transmitter was mounted inside the module in front of the window made of special glass and having a diameter of 400 mm. To protect the photoreceiving block from rereflected sensing radiation, the optical axis of the transmitter was turned by 1.5° relative to the window axis. The Galilei telescope served as optical antenna of the transmitter, and the Mangin mirror-lens telescope with external reflecting covers served as the receiving antenna. All this allowed an essential decrease of the telescope linear size.

The "cold" and "hot" reservation of some lidar blocks was used to increase the reliability of the instrumentation, as it was customary in space instrument-making. Two photoreceiving channels were simultaneously in "hot" reserve, i.e., in continuous operation. "Cold" reserve included the recording system and the laser block.

Identical YAG lasers with a frequency doubling were used in the lidar. They formed two transmitting channels, main and reserve, which were switched automatically. The photomultiplying tube PMT-84, having a high quantum efficiency in the visible wavelength range and the best parameters for operation in the analog mode, was used as an optical detector. Two photomultipliers worked simultaneously; to increase their efficiency, the total-reflection prisms were fastened to their ends. The lidar signals after photoelectric transformation entered the recording system consisting of two independent channels, range-meter (amplitude – distance) and lidar (distance – amplitude). The first channel provided for measurements of the time interval between the moments of emitting and receiving the return signal reaching some threshold value. The analog-to-digital converter with a digitizing rate of 20 ns was used in the lidar channel. The amplitude sample of the signals was recorded into the memory, where the data strings were formed, which then were transmitted by the station-based computer to the Mission Control Center for the consequent decoding and processing.

Measurements with the use of the spaceborne lidar "BALKAN" were carried out in 1995–1996 during three space expeditions of cosmonauts SE-19 – SE-21. The lidar work was terminated in June, 1996 because of the crash of the module "Spektr", although only less then 10% of its resource was used to the moment. Preliminary results of investigation[13] enabled the technological testing of the lidar, elaboration of the techniques for joint under-satellite experiment, and receiving the arrays of lidar signals feasible for testing the algorithms of the sensing data processing.

Interpretation of the lidar data of the cloudiness space sensing

The purpose of the space measurements is to obtain data on the global distribution of cloud and aerosol

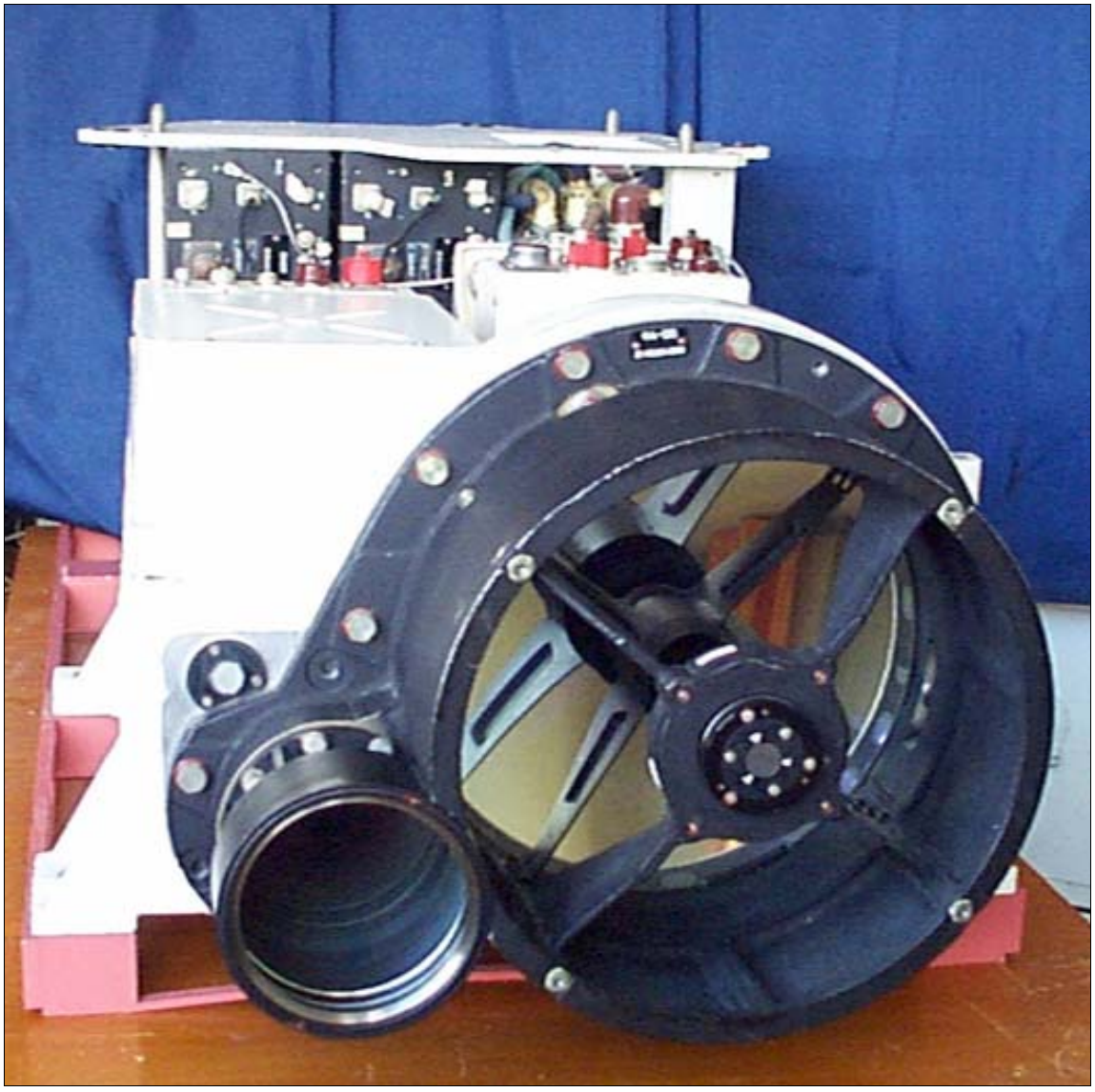

Fig. 1. Design of the receiver-transmitter device of the spaceborne lidar "BALKAN."

fields over the Earth surface. The lidar is capable of identifying the scattering layer (aerosol/cloud), its position (height/thickness), and phase composition (ice and/or water). Proper retrieval of the optical parameters, i.e., the extinction and backscattering coefficients, optical thickness, depolarization and lidar ratios, at the working lidar wavelengths (355/532/1064 nm under LITE program and 532/1064 nm plus depolarization at 532 nm for CALIPSO) is the key moment in solving the aforementioned problems (see, for example, Refs. 14 and 15).

Interpretation of the lidar space signals has some peculiarities connected with great sensing distances and, hence, high multiple scattering (MS) background. The background appears due to formation of great scattering volumes within the lidar sensing cone, when the transversal sizes of the light beam at the cloud top turned to be comparable with the thickness of the sensed cloud layer. The radiation scattered in sideward directions practically does not go out of the receiver field of view and participates in the consequent formation of the reflected light flow.[16,17]

Thus, interpretation of the signals is an ill-posed problem, because it requires *a priori* information on the scattering phase function (on the scattering matrix at polarization measurements). Its solution is complicated by the absence of a universal analytical model, describing the contribution of scattering at multiplicities exceeding 2, and of general models of polydispersion scattering matrices for clouds of crystal and mixed phase composition.

There are two ways of data interpretation: correction of the MS background and conversion of signals by traditional methods[18,19] or retrieval of data immediately from the signal fraction determined by MS. In any case, the first stage of interpretation is the construction of an adequate mathematical model, describing the lidar signal with accounting for the MS contribution. The doubtless way for its accounting for is a solution of the non-stationary transfer equation by the Monte Carlo method (the most complete review of the methods for remote sensing is presented in Ref. 17). A disadvantage of this approach is a poor automation, especially well seen at the processing of great amounts of lidar measurements. This stimulated the development of methods for "quasi-analytical" approximation of the MS background.[20,21] Our model falls in this field of investigations.

The state of polarization of linearly polarized radiation is described, as is known, by the Stokes parameter vector:

$$\begin{pmatrix} S_1(z) \\ S_2(z) \\ S_3(z) \\ S_4(z) \end{pmatrix} = \begin{pmatrix} F_{\parallel}(z) + F_{\perp}(z) \\ F_{\parallel}(z) - F_{\perp}(z) \\ 0 \\ 0 \end{pmatrix},$$

where $F_{\parallel}(z)$ is the parallel and $F_{\perp}(z)$ is the perpendicular components of the backscattering signal. A relatively simple model was proposed[22,23] for the first component of the Stokes parameter vector (radiation intensity), taking into account the MS contribution and used for interpretation of the ground-based measurements:

$$S_1(z) = S_1^{(1)}(z)\exp\left\{2\int_{z_0}^{z}\left[\sigma(z')\left(1-\eta_1(z')\right)\right]\mathrm{d}z'\right\}, \quad (1)$$

where $S_1^{(1)}(z)$ is the component caused by the single scattering; $\sigma(z)$ is the radiation extinction coefficient;

$$\eta_1(z) = 1 - \frac{\ln\left\{S_1(z)/S_1^{(1)}(z)\right\}}{2\tau(z)} = 1 - \frac{m_1(z)}{2\tau(z)},$$

$$\tau(z) = \int_{z_0}^{z}\sigma(z')\,\mathrm{d}z', \quad \eta_1 \in]0,\,1[, m_1(z)$$

depends on the scatterer type and is determined by combination of the elements of the scattering matrix.[24] It was shown[25,26] that the analogous model is also true for the second component of the Stokes parameter vector:

$$S_2(z) = S_2^{(1)}(z)\exp\left\{2\int_{z_0}^{z}\left[\sigma(z')\left(1-\eta_2(z')\right)\right]\mathrm{d}z'\right\}, \quad (2)$$

where

$$\eta_2(z) = 1 - \frac{\ln\left\{S_2(z)/S_2^{(1)}(z)\right\}}{2\tau(z)} = 1 - \frac{m_2(z)}{2\tau(z)},$$

$\eta_2 \in]0,1[, m_2(z)$ also depends on the elements of the scattering matrix.[26] The results of calculation of the η_1 by the Monte Carlo method for different scattering matrices[26] have shown that at great sensing distances

$$\eta_1(z) \cong \text{const}; \ \eta_2(z) \cong \text{const}.$$

The values of these parameters are completely determined by the type of scatterers.

Thus, the models (1) and (2) are applicable for interpretation of spaceborne measurements. Moreover, it was shown[26] that

$$\eta_1(z)/\eta_2(z) \cong \text{const},$$

and that characteristics of polarization of the lidar signals at long sensing distances depend on the lidar ratio and the integral of the functions, stipulated by combination of elements of the scattering matrix. Angular differences in the elements of the scattering matrix, essential for different types of crystals are not determining at spaceborne sensing. The latter conclusion is very important for interpretation of the signals, because it essentially decreases the amount of *a priori* data, necessary for their conversion relative to the optical parameters.

The results of retrieval of the extinction coefficient based on the proposed approach are presented below. The MS background was considered in calculations as the noise, it was described by the

model (1) and corrected by iterative algorithm.[24] The results exemplify joint interpretation of spaceborne and airborne measurements and can very well exemplify the synchronization of lidar measurements from different carriers. We used the sensing data in the framework of the LITE program (below "L") and the data of under-satellite measurements by the German airborne lidar ALEX (Airborne Lidar EXperiment,[27] below "A") on September 14, 1994 (orbit 79), at $\lambda = 532$ nm. These data were kindly presented by Space Agencies of USA and Germany. From the flight trajectory, the sensing part was selected (8÷9.2°E and 56.9°N) containing both water (the height $z = 4.9$–8 km, Fig. 2) and crystal clouds ($z = 8.9$–12 km, Fig. 3); measurement time was 19:16:00÷19:16:10 (UTC) for the lidar "L" and 19:10:08÷19:04:22 (UTC) for the lidar "A" (the aircraft and the satellite flew in opposite directions). The array of measurements by the lidar "L" consisting of 100 signals in 800 m intervals in horizontal direction corresponded to this part; for comparison, the data array of the airborne lidar was also transformed to 100 signals, each being averaged over 21 shots (within the spot of sensing by the lidar "L") in 800 m intervals.

Two-dimensional distributions of the extinction coefficients obtained by the lidar "A" are presented in Figs. 2*a* and 3*a*, and the data by the lidar "L" are shown in Figs. 2*b* and 3*b*. Corresponding maximal values of the optical thickness τ_{max} (Figs. 2*c* and 3*c*) and the extinction coefficient σ_{max} (Figs. 2*d* and 3*d*) were obtained along the flight path.

Analysis of the results shows that the spaceborne signals from dense clouds (see Fig. 2) give more extensive data on their optical characteristics as compared to ground-based (airborne) measurements, however, removal of the MS background from the total signal in the processing is not expedient in this case. The extraction of the data contained in the MS background by the Monte Carlo method[28] or by the use of the diffuse approximation[29] makes it possible to use space signals for determination of such parameters of dense clouds, which cannot be obtained by other lidar measurements.

Removal of the MS noise from the lidar signal and its processing by the methods developed in the single scattering approximation is admissible for cirrus and optically thin water clouds (see Fig. 3). However, only adequate description of the MS background is insufficient. The magnitude of the MS contribution depends on the scattering matrix, which is unknown *a priori* and, generally speaking, should be determined from the signals themselves. The problem of *a priori* uncertainty in selection of the scattering matrix is, probably, the most complicated problem in the interpretation of the sensing data.

This is evidently seen from the necessity of *a priori* setting the lidar ratio for retrieval of optical parameters of a two-component medium. A complete solution of the inverse problem is possible only for Raman sensing.[30] Note that selection of the scattering matrix for water clouds in processing the spaceborne signals is not of importance, because the variability range of the lidar ratio is small, the matrices are close to each other, and retrieval of the parameters in the presence of the MS background is stable.[28] The use of polarization characteristics of radiation seems more promising for cirrus clouds.

Using the models (1) and (2), one can show that logarithmic derivative from the profile of polarization (the ratio of the Stokes vector second component to the first one) is proportional to the profile of the lidar ratio multiplied by the backscattering coefficient.[26] This allows one to simultaneously retrieve the profile of depolarization and lidar ratios, as well as the extinction (or backscattering) coefficient from polarization measurements, and to estimate the type and size of scattering particles with a definite degree of reliability. The range of application of the method is restricted by adequacy of the mathematical model describing the processes of multiple scattering; and the main difficulty is the necessity of correct numerical differentiation of the ratio of two experimentally measured functions.

Studying possible errors in determination of optical parameters of crystal clouds and aerosol, appeared under conditions of *a priori* uncertainty in the type of scatterers, authors of Ref. 31 have drown the following conclusions:

First, the profile of lidar ratio is stable to the retrieval with "erroneous" scattering matrix; second, *a priori* uncertainty leads to opposite distortions when determining the extinction coefficient by the method of logarithmic derivative or the iterative method, so it is expedient to estimate $\sigma(z)$ by the both methods, because large discrepancies explicitly point to the "erroneous" matrix used in the processing.

Under-satellite lidar observations

The important part of lidar observations connected with their validation is organization of synchronous measurements of the optical parameters of aerosol and cloud fields using airborne and ground-based tools in the region of the satellite flight. The first large-scale experience of such escort is connected with the program ELITE-94 [Ref. 32], in which 17 European lidar stations were involved, including two airborne lidars. The airborne data obtained by one of them, the German lidar ALEX [Ref. 27] were presented in previous Section of the paper.

To calibrate the data of the spaceborne lidar CALIPSO, the special international program QPQ was organized,[33] for realization of which practically all available regional and international atmospheric measurement networks of the planet were attracted. The Institute of Atmospheric Optics is the head organization in Russia in coordination of operation of all Russian lidars. It should be noted that the lidar CALIPSO is a part of a large group (A-train) of spaceborne instruments consisting of the satellites "Aqua," "CloudSat," CALIPSO, PARASOL, and

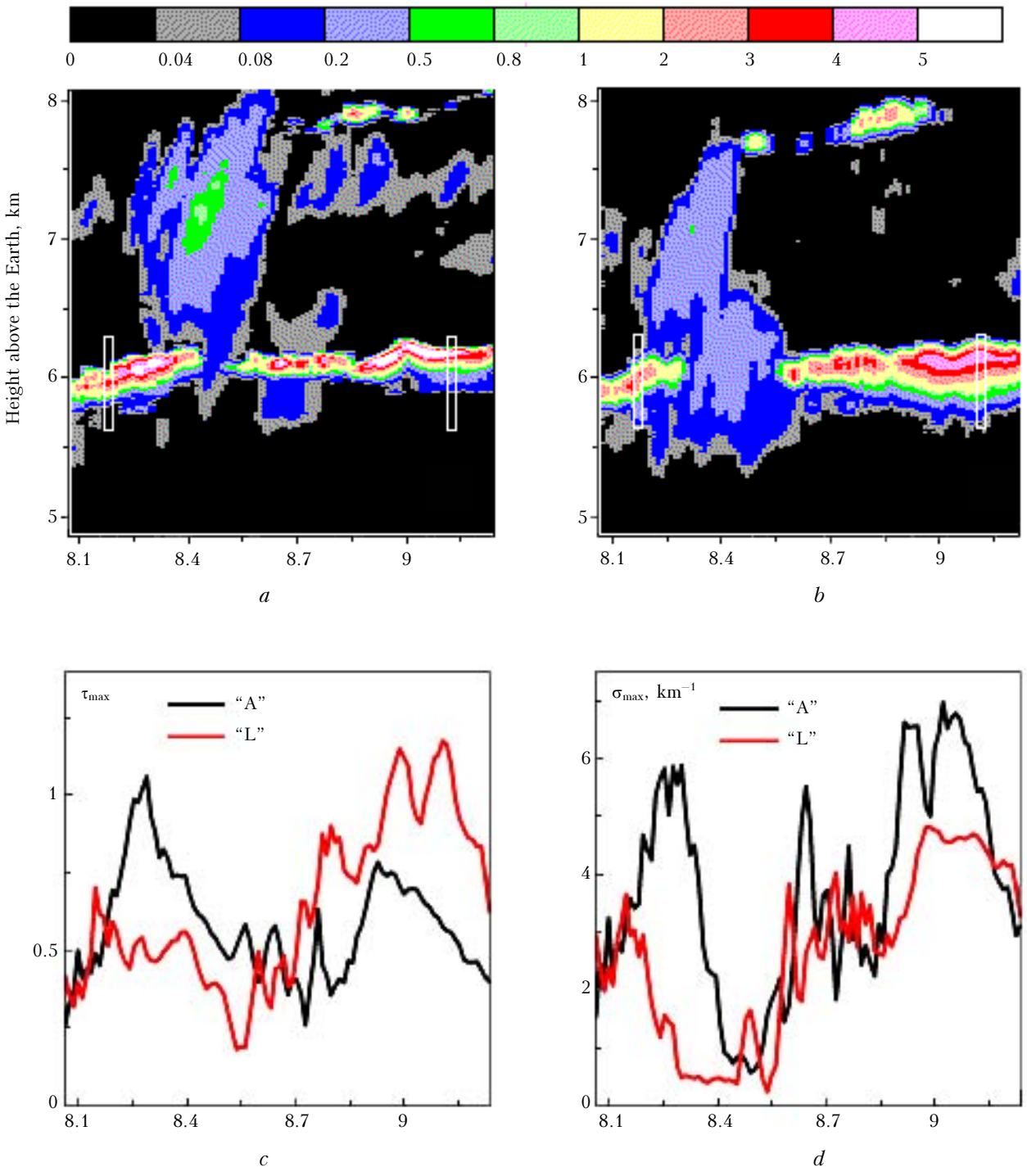

Fig. 2. Retrieval of optical parameters of water clouds on the data from synchronous sensing by spaceborne and airborne lidars on September 14, 1994 (orbit 79): extinction coefficient (1/km) on data "A" (*a*) and data "L" (*b*); maximal optical thickness (*c*) and extinction coefficient (*d*) along the flight path.

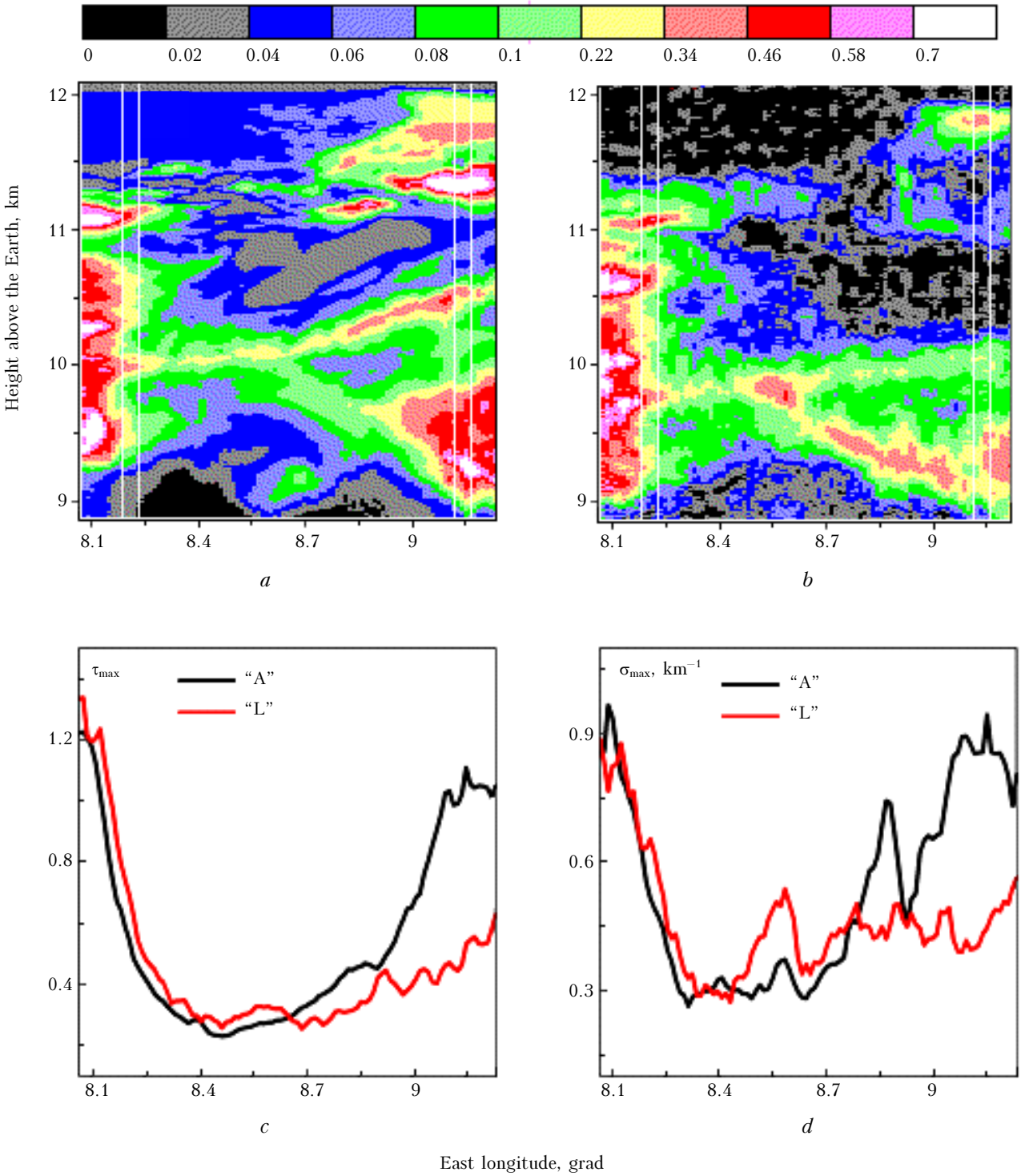

Fig. 3. Retrieval of optical parameters of crystal clouds on the data from synchronous sensing by spaceborne and airborne lidars on September 14, 1994 (orbit 79): extinction coefficient (1/km) on data "A" (*a*) and data "L" (*b*); maximal optical thickness (*c*) and extinction coefficient (*d*) along the flight path.

"Aura." The time interval of operation between them varied from tens of seconds to minutes.

Cloud and aerosol fields have different spatial and temporal scales, so different strategy for validation of the satellite data is planned. Aerosol fields usually have a greater spatial correlation then cloud ones and provide for a better comparison between the ground-based and space observations. According to recommendations of the program, the distance between position of the ground-based lidar and projection of the CALIPSO trajectory can reach 50–100 km.[33] Optical properties of cloud fields have more significant horizontal spatial variability, which for cirrus clouds can reach[33] 100% at the distances up to 5 km. So, in the best case, statistical analysis is applicable here. Correlation distances for estimation of the cloud phase composition (ice/water) reach ~ 50 km, therefore, they can be sufficient for direct comparison. Note that the ground-based lidars of high spectral resolution (HSRL) and Raman lidars are preferable for monitoring both aerosol and cloud fields.

In this Section, some results are presented, which were obtained during Siberian forest fires in 2006 with stationary multi-wavelength lidar "LOZA-S" of IAO SB RAS [Ref. 34] and the lidar CALIPSO. Fires of Siberian boreal forests are the permanent source of aerosol and gas admixtures in the atmosphere, and their consequences have a global character because of large scale propagation of smoke plumes. Suffice it to say that the products of vast Siberian fires were observed by lidar stations in the troposphere of both Central Europe[35] and Asia.[36,37] Pollutants were transported in two directions. One part of admixtures was transported by air masses directly to Europe. Easterly transfer favored the appearance of smoke layers in the troposphere over Japan, Korea, North America and then again over Europe and Siberia, enclosing a 17-day period of global transfer.[35] Spatial-temporal dynamics of the development of smoke "clouds," as well as their optical and microphysical parameters were determined by means of the lidars.[35–37]

The episode of lidar observations presented below is related to July, 2006, in the second half of which smoke admixtures from forest fires in the Krasnoyarskii Krai were observed in the atmosphere over Tomsk. This follows from analysis of the motion of air masses by the method of back trajectories (Fig. 4*a*). General image of smoke in the atmosphere over Tomsk Region on July 21, 2006 is seen in the picture obtained from the satellite TERRA-MODIS (Fig. 4*b*). These data are available on the web-site http://aeronet.gsfc.nasa.gov.

The results of spaceborne sensing in this and previous periods are shown in Fig. 5 as the characteristic "red" cloud at heights from 0.5 to 3 km.

Omitting the sensing results for the next days, the space lidar images allow one to trace both vertical structure of the smoke plume and the spatial tendency of its movement (web-site http://www.calipso.larc.nasa.gov/products/lidar).

The data of ground-based observations by means of the lidar at a wavelength of 532 nm for the considered period are shown in Fig. 6.

Vertical profiles of the backscattering coefficient and the lidar ratio are shown (for comparison, the data, obtained on July 4 under background conditions, are presented). Aerosol structures of the lower 4-km layer of the troposphere in the period of July 17–21, i.e., in the period of arrival of smoke admixtures, essentially differ from the aerosol structure on July 4. In the initial period (July 17–19) the main amount of aerosol particles is observed between 2 and 4 km as individual layers, then the maximum filling of the boundary layer by admixtures up to the height of 2.5 km, as well as homogeneous filling of the troposphere by aerosol occur on July 21. The last day, according to the data of the AERONET site, the value of the atmosphere optical thickness ($\lambda = 500$ nm) reaches 1.32 and becomes more than 3 times greater than in the initial period of the experiment (July 17, 2006).

In fact, the difference in lidar data for these days is more significant, if consider also the lower 2.5-km high layer of the atmosphere. The ratio of the aerosol backscattering coefficients at the top of the selected height range reaches 5. On the average, the values of the backscattering coefficient of the smoke filling the lower troposphere (1–3 km) in the considered period vary between 1 and 10 $Mm^{-1} \cdot sr^{-1}$, which is in agreement with the results of other observations.

It is also interesting to compare the data on the lidar ratio, the value of which characterizes microstructural variations of aerosol parameters and does not depend on the particle concentration. This optical parameter was measured only in the nighttime, because it was calculated based on the signals of the lidar Raman channel.[34] Its value for the background atmosphere (July 4, 2007) lies in the range 50–55 sr, while the value of lidar ratio for the "smoke" areas of the atmosphere represented by observations on July 18 and 20 increases to 75–80 sr. Somewhat smaller values were obtained in Ref. 36, but the tendency in the differences is the same. Therefore, together with the degree of radiation depolarization, the lidar ratio is one of the main information signs for selection of smoke aerosol. On the whole, the results obtained by all ground-based instruments (lidar, AERONET, photometer) satisfactory agree with each other.

The same can be related to comparison of the data of ground-based and spaceborne lidars presented on the site http://calipsovalidation.hamptonu.edu/Data_Catalog/ (user password is required).

The considered episode of joint observations is a clear evidence of the capabilities of the modern lidar techniques. Accounting for photometric and multi-wavelength lidar observations as well, the statement of the retrieval problem for the vertical profile of the aerosol particle microstructure is justified.[35–38]

In conclusion, authors would like to thank the specialists of the Special Design Bureau "Optika" and

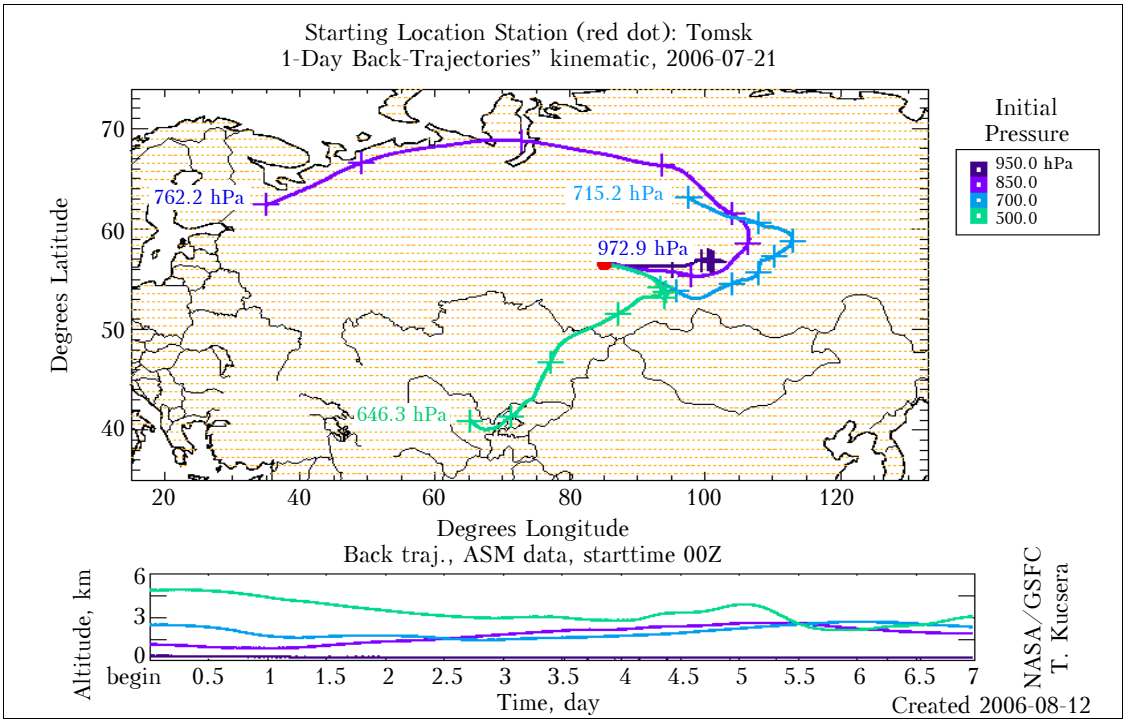

a

b

Fig. 4. Trajectory of air masses motion (*a*) and image of smoke in the atmosphere over Tomsk Region (*b*) on July 21, 2006 from the satellite TERRA-MODIS data.

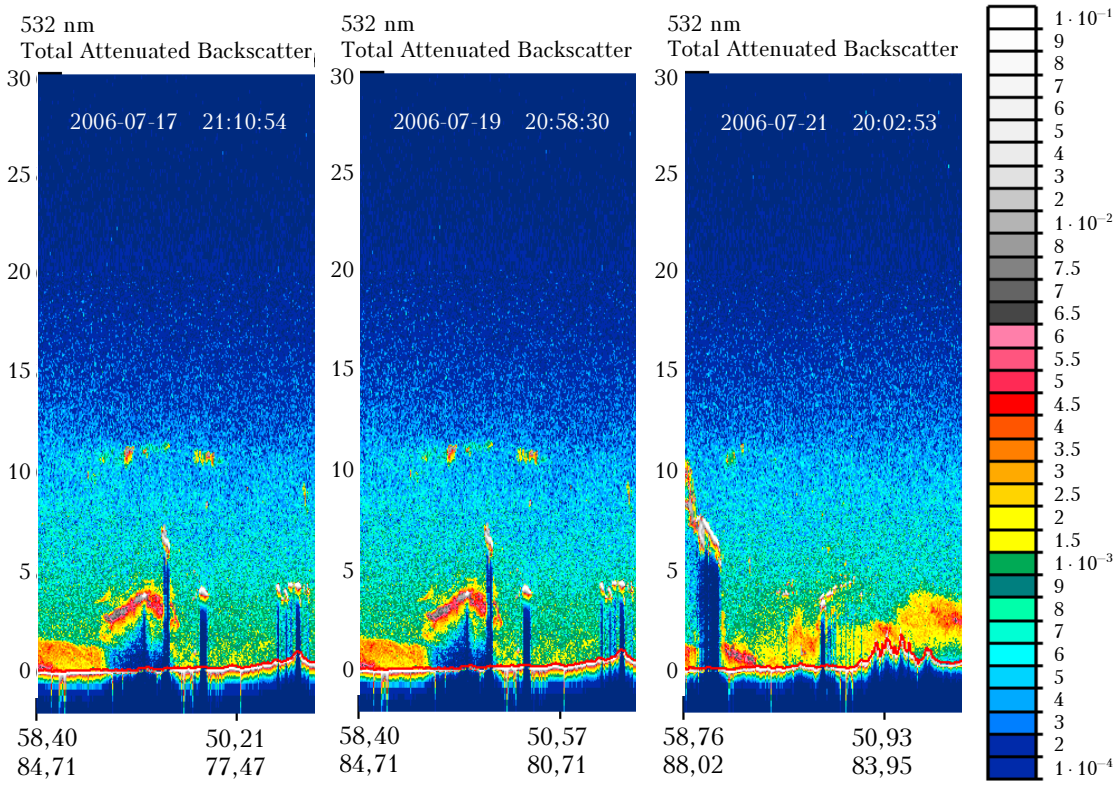

Fig. 5. Dynamics of evolution of smoke cloud over Tomsk Region on July 17–21, 2006 from spaceborne lidar "CALIPSO" data. *X*-axis: upper line denotes latitude, lower one – longitude. Color scale of range of backscattering coefficients ($km^{-1} \cdot sr^{-1}$) is presented on the right. Measurement time was in UTC system.

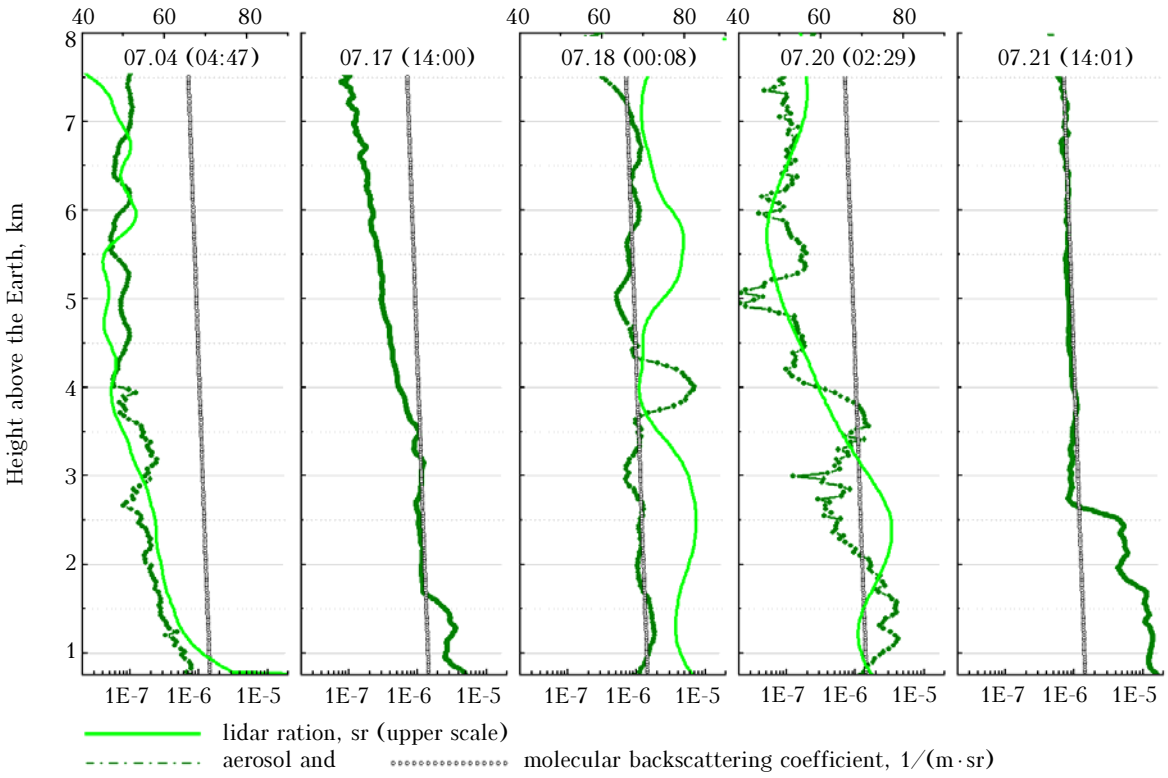

Fig. 6. Variation dynamics of optical parameters vertical profiles over Tomsk in the period of forest fires on July, 2006. The lidar LOZA-S data were used.

the Laboratory OZA IAO SB RAS for great contribution to creation of the spaceborne lidar "BALKAN."

Acknowledgements

It is also necessary to note that investigations in the field of laser sensing were permanently supported by both Russian Foundation for Basic Research (Grants Nos. 94–05–16461; 98–05–64066; 02–05–64486; 05–05–39014; 05–05–97240; 06–05–89500; 07–05–91102; and 07–05–00672) and International Scientific Foundations (CRDF Nos. RG2-2357 and RG-2871; INTAS No. 01-0239; ISTC No. B-1063; TNSC No. RP06N06).

References

1. S. McDermid and the NDACC Lidar Working Group, in: *Reviewed and Revised Papers Presented at the 23rd Int. Laser Radar Conf.* Nara, Japan (2006), pp. 665–666.
2. E.J. Welton, J.R. Campbell, T.A. Berkoff, J.D. Spinhirne, S.-Ch. Tsay, B. Holben, and M. Shiobara, in: *Reviewed and Revised Papers Presented at the 21st Int. Laser Radar Conf.* Quebec, Canada (2002), pp. 285–288.
3. G. Pappalardo, J. Bösenberg, A. Amodeo, A. Ansmann, A. Apituley, D. Balis, Ch. Böckmann, A. Chaikovsky, A. Comeron, V. Freudenthaler, G. Hansen, V. Mitev, A. Papayannis, M.R. Perrone, A. Pietruczukl, M. Pujadas, F. Ravetta, V. Rizi, V. Simeonov, N. Spinelli, D. Stoyanov, Th. Trickl, and M. Wiegner, in: *Reviewed and Revised Papers Presented at the 23rd Int. Laser Radar Conf.* Nara, Japan (2006), pp. 667–670.
4. T. Murayama, N. Sugimoto, I. Uno, K. Kinoshita, K. Aoki, N. Hagiwara, Z. Liu, I. Matsui, T. Sakai, T. Shibata, K. Arao, B.-J. Shon, J.-G. Won, S.-C. Yoon, T. Li, J. Zhou, H. Hu, M. Abo, K. Iokibe, R. Koga, Y. Iwasaka, J. Geophys. Res. D **106**, No. 16, 18346–18359 (2001).
5. R.M. Hoff, K.J. McCann, B. Demoz, J. Rechardt, D.N. Whiteman, T. McGee, M.P. McCormick, C.R. Philbrick, K. Strawbridge, F. Moshary, B. Gross, S. Ahmed, D. Venable, and E. Joseph, in: *Reviewed and Revised Papers Presented at the 21st Int. Laser Radar Conf.* Quebec, Canada (2002), pp. 281–284.
6. J.C. Antuña, M. Andrade, E. Landulfo, B. Clemesha, E. Quel, and A. Bastidas, in: *Reviewed and Revised Papers Presented at the 23rd Int. Laser Radar Conf.* Nara, Japan (2006), pp. 673–676.
7. A. Chaikovsky, A. Ivanov, Yu. Balin, A. Elnikov, G. Tulinov, I. Plusnin, O. Bukin, and B. Chen, in: *Reviewed and Revised Papers Presented at the 23rd Int. Laser Radar Conf.* Nara, Japan (2006), pp. 671–672.
8. E.V. Browell, in: *Conf. Abstracts of 9th Int. Laser Radar Conf.* Munich (1979), pp. 176–177.
9. D.M. Winker, J. Pelon, and M.P. McCormick, in: *Reviewed and Revised Papers Presented at the 23rd Int. Laser Radar Conf.* Nara, Japan (2006), pp. 991–994.
10. Yu.S. Balin, V.V. Burkov, I.V. Znamenskii, V.E. Zuev, V.I. Efimkin, V.S. Il'ichevskii, V.E. Mel'nikov, I.V. Samokhalov, V.N. Sobolev, and A.A. Tikhomirov, in: *Abstracts of Papers of 15 Int. Laser Radar Conf.* Tomsk, Part I (1990), pp. 12–14.
11. Yu.S. Balin, I.V. Znamenskii, V.E. Zuev, V.E. Mel'nikov, S.V. Samoilova, and A.A. Tikhomirov, Atmos. Oceanic Opt. **8**, No. 9, 711–717 (1995).
12. Yu.S. Balin, I.V. Znamenskii, V.E. Mel'nikov, and A.A. Tikhomirov, Atmos. Oceanic Opt. **9**, No. 3, 231–234 (1996).
13. Yu.S. Balin, A.A. Tikhomirov, and S.V. Samoilova, Atmos. Oceanic Opt. **10**, No. 3, 209–220 (1997).
14. C.M.R. Platt, D.M. Winker, M.A. Vaughan, and S.D. Miller, J. Appl. Meteorol. **38**, Is. 9, 1330–1345 (1999).
15. S.A. Young, *CSIRO Atmospheric Research Technical Paper* (Commonwealth Scientific and Industrial Research Organization, Collinwood, Victoria, Australia), No. 54, 3–28 (2002).
16. G.M. Krekov, M.M. Krekova, and I.V. Samokhvalov, Issled. Zemli iz Kosmosa, No. 6, 77–83 (1986).
17. L.R. Bissonnette, P. Bruscaglioni, A. Ismaelli, G. Zaccanti, A. Cohen, Y. Benayahu, M. Kleiman, S. Egert, C. Flesia, P. Schwendimann, A.V. Starkov, M. Noormohammadian, U.G. Oppel, D.M. Winker, E.P. Zege, I.L. Katsev, and I.N. Polonsky, Appl. Phys. B **60**, 355–362 (1995).
18. F.G. Fernald, Appl. Opt. **23**, No. 5, 1609–1613 (1984).
19. V.A. Kovalev, Appl. Opt. **32**, No. 30, 6053–6065 (1993).
20. E.P. Zege, I.L. Katsev, and I.N. Polonsky, Appl. Phys. B **60**, 345–353 (1995).
21. G.H. Ruppersberg, M. Kerscher, M. Noormohammadian, U.G. Oppel, and W. Renger, Beitr. Phys. Atmos. **70**, 93–105 (1997).
22. V.E. Zuev, G.M. Krekov, M.M. Krekova, and I.E. Naats, in: *Problems of Laser Sensing of Clouds* (Nauka, Novosibirsk, 1976), pp. 3–33.
23. C.M.R. Platt, J. Atmos. Sci. **38**, Is. 1, 156–167 (1981).
24. Yu.S. Balin, S.V. Samoilova, M.M. Krekova, and D.M. Winker, Appl. Opt. **38**, No. 30, 6365–6373 (1999).
25. D.M. Winker, Proc. SPIE **5059**, 128–139 (2003).
26. S.V. Samoilova, Yu.S. Balin, M.M. Krekova, and D.M. Winker, Appl. Opt. **44**, No 17, 3499–3509 (2005).
27. W. Renger, C. Kiemle, H.-G. Schreiber, M. Wirth, and P. Moerl, in: *Final Results Workshop Proc.* (IROE-CNR, Florence, Italy, 1995), pp. 15–30.
28. U.G. Oppel, Proc. SPIE **4341**, 237–250 (2000).
29. A.B. Davis, S.P. Love, R.F. Cahalan, M.J. McGill, D.M. Winker, and M.A. Vaughan, in: *Proc. of 21th Lidar Remote Sensing in Atmospheric and Earth Sciences,* Part II. Quebec, Canada (2002), pp. 499–501.
30. A. Ansmann, U. Wandinger, M. Reibessel, C. Weitcamp, and M. Michaelis, Appl. Opt. **31**, No. 33, 7113–7131 (1992).
31. S.V. Samoilova and M.M. Krekova, Atmos. Oceanic Opt. **18**, No. 10, 822–830 (2005).
32. P.A. Fletcher and E. Attema, *ELITE-94: The European Lidar In-space Technology Experiment campaign overview. Final Results Workshop Proc.* (IROE-CNR, Florence, Italy, 1995), 109 pp.
33. QPQ validation website http://calipsovalidation.hamptonu.edu
34. S.V. Samoilova, Y.S. Balin, A.D. Ershov, G.P. Kokhanenko, and I.E. Penner, in: *Proc. of Int. Workshop ISTC "BAIKAL-2006": Irkutsk, Russia* (2006), pp. 57–59.
35. I. Mattis, D. Muller, A. Ansmann, U. Wandinger, T. Murayama, and R. Damoah, in: *Reviewed and Revised Papers Presented at the 22nd Int. Laser Radar Conf.* Matera, Italy (2004), pp. 857–860.
36. T. Murayama, K. Wada, D. Müller, and T. Tsukamoto, in: *Reviewed and Revised Papers Presented at the 22nd Int. Laser Radar Conf.* Matera, Italy (2004), pp. 365–368.
37. Ch.H. Lee, J.H. Kim, Ch.B. Park, A. Shimizu, I. Matsui, and N. Sugimoto, in: *Reviewed and Revised Papers Presented at the 22nd Int. Laser Radar Conf.* Matera, Italy (2004), pp. 535–538.
38. A. Chaikovsky, A. Bril, V. Barun, O. Dubovik, B. Holben, A. Thompson, P. Goloub, and P. Sobolewski, in: *Reviewed and Revised Papers Presented at the 22nd Int. Laser Radar Conf.* Matera, Italy (2004), pp. 345–348.